

## Small Signal Modeling Of Controller For Statcom Used In Distribution System For Reactive Power Management

Wahiddun Nisa, P.Sunita

<sup>1</sup>M. Tech, Dept. of EEE Centurion University of Technology & Management Paralakhemundi, India

<sup>2</sup>Associate Professor, Dept. of EEE Centurion University of Technology & Management Paralakhemundi, India

### ABSTRACT

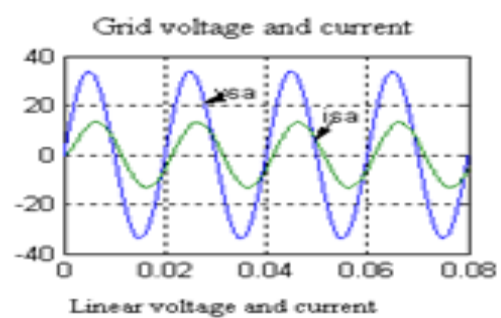
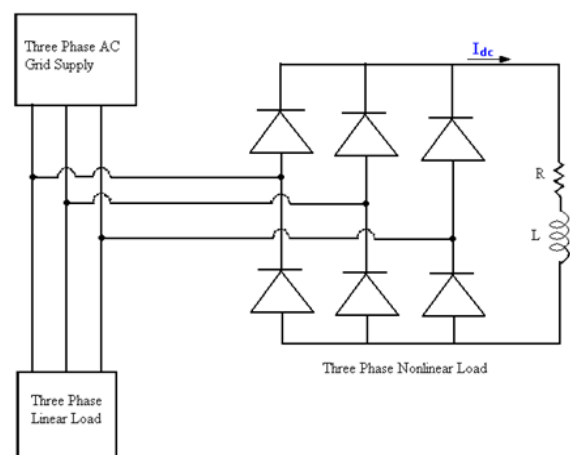
In this paper non-linear model of the STATCOM is linearized and the following strategies have been adopted . Hence, a small signal model is adopted here. Here, the grid voltage lags the fundamental component of the STATCOM converter terminal voltage with a phase angle difference ' $\alpha$ '. Small signal modeling of the phase angle ' $\alpha$ ' and modulation index ' $m$ ' is also done. A single PI-controller for the reactive component current of the STATCOM has been designed. In this model, the DC-link capacitor voltage is held constant without using a separate controller. The STATCOM are designed using SVPWM technique. Through adjustment of the modulation index, fast modulation of the STATCOM reactive power output can be achieved due to high sensitivity of the same with respect to the output voltage of the STATCOM VSC. The model, with PI controllers has been simulated in MATLAB/SIMULINK environment with variation of the pre-charge voltage on the DC-link capacitor with linear loads (inductive). Improvement of the power factor of the grid current is achieved for linear loads.

**Keywords:** -PHASE ANGLE, PI, MODULATION INDEX, SVPWM

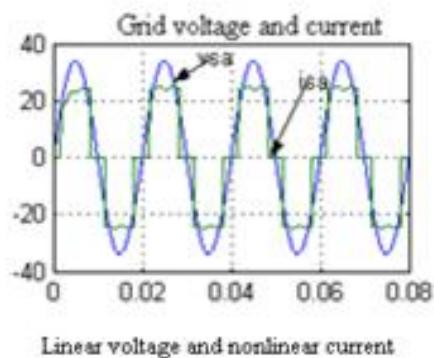
### I. INTRODUCTION

Reactive power surplus/deficit causes a precarious condition leading to voltage collapse. Hence, the electrical utilities and heavy industries are facing a number of challenges related to reactive power management [1-5]. Reactive power (VAR) compensation is defined as the management of reactive power to improve the performance of ac power systems. The concept of reactive power compensation embraces wide and diverse fields of both systems and customer problems, especially related to the phenomena like voltage unbalance, distortion or flicker [6] on the electrical grid, voltage sags [7-8], poor power factor or even voltage instability [9-11].

The loads are generally categorized as linear and non-linear loads. The linear loads are  $R$ ,  $R - L$ ,  $R - L - C$ , motors, heaters and incandescent lamps while non-linear loads are power electronic apparatus like diodes or thyristor rectifiers, switched mode power supply (SMPS), adjustable speed drives, ferromagnetic devices, arcing equipments, induction heating systems etc. As is well known, the current is proportional to the voltage in case of a linear load as shown in Fig.1. (a) Whereas the current is not proportional to the voltage in case of non-linear load (as shown in Fig.1. (b)).



(a)



(b)

Fig.1. Linear and non-linear load connected to grid supply

Series and shunt VAR compensation techniques are used to improve electrical performance of ac power systems. Series compensation modifies the transmission or distribution system (reflected) parameters, while shunt compensation changes the equivalent impedance of the load.

Earlier, rotating synchronous condensers and fixed or mechanically switched capacitors (or inductors) were used for shunt compensation [12, 13]. However, in recent years [14], static VAR compensators employing thyristor switched capacitors and thyristor controlled reactors have been developed. Also, the use of self-commutated PWM converters with an appropriate control scheme permits the implementation of static compensators with a response time faster than the fundamental power cycle

## II. OPERATING PRINCIPAL

The STATCOM (shown in Fig.2) consists of a controlled solid-state device based voltage source converter connected in parallel to the power system through an ac-side reactor and a capacitor on the DC-link side (which has to be maintained at a given voltage under closed-loop control). It is the static analogue of a synchronous motor operating at no load with over excitation (synchronous condenser). This equipment, however, has no mechanical inertia. It is well understood that the STATCOM operates in capacitive mode when its output voltage is greater than the grid side voltage (when it has to compensate for inductive loads), whereas in the reverse case, it works to compensate for capacitive loads.

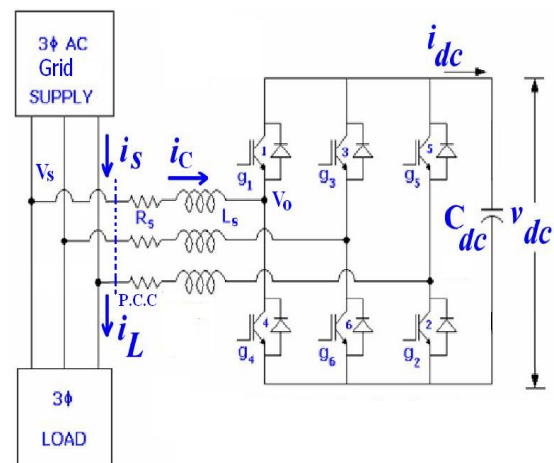


Fig.2 Schematic diagram of the STATCOM

As mentioned already, the STATCOM is, in principle, a static (power electronic) replacement of the age-old synchronous condenser as shown in Fig.2. It shows the schematic diagram of a STATCOM connected to the utility grid at the point of common coupling (PCC) through the coupling inductors (or ac side reactors). The phasor diagram of the fundamental component of the STATCOM converter terminal voltage and the grid voltage at PCC for an inductive load in operation, (neglecting the harmonic content in the STATCOM converter terminal voltage) is presented in Fig.3 (a). However, the inter-connecting reactors have fundamental power frequency voltage at one end and PWM voltage waveform of a converter at other end. The fundamental component of the converter terminal voltage,  $V_{o1}$ , may be forced to be in-phase with the sinusoidal grid voltage,  $V_s$ , under closed-loop control. Increasing the amplitude of the STATCOM converter terminal voltage,  $V_{o1}$ , above the amplitude of the grid voltage,  $V_s$  causes leading (capacitive) current,  $I_{c1}$ , to be drawn from the grid as shown in Fig.3(b) and similarly decreasing  $V_{o1}$  below  $V_s$  causes lagging (inductive) current to be drawn from the grid. However, if  $V_{o1}$  is strictly kept in phase with  $V_s$ , no active power flows from the grid side to the STATCOM to provide for its losses. Therefore,  $V_{o1}$  must be made to lag  $V_s$  appropriately so that the STATCOM draws adequate but not excess active power from the grid to make up for the losses.

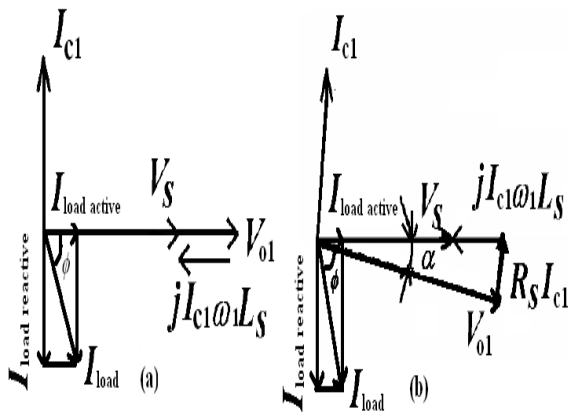


Fig.3. Schematic phasor diagram for operation of STATCOM

### III. SVPWM

#### Principle of Pulse Width Modulation (PWM)

A circuit model of a single-phase inverter with a centre-taped grounded DC bus is illustrated in Fig.4. Fig.5 illustrates the principle of pulse width modulation. It is depicted from Fig.5, the inverter output voltage is determined in the following:

$$\text{When } V_{control} > V_{tri}, V_{ao} = \frac{V_{dc}}{2} \quad (1)$$

$$\text{When } V_{control} < V_{tri}, V_{ao} = -\frac{V_{dc}}{2} \quad (2)$$

The inverter output voltage has the following features:

- PWM frequency is the same as the frequency of  $V_{tri}$ .
- Amplitude is controlled by the peak value of  $V_{control}$ .
- Fundamental frequency is controlled by the frequency of  $V_{control}$ .

Modulation index ( $m$ ) is defined as

$$m = \frac{v_{control}}{v_{tri}} = \frac{(V_{ao})_1}{V_{dc}/2} \quad (3)$$

Where,  $(V_{ao})_1$  is the fundamental frequency component of peak of  $V_{ao}$

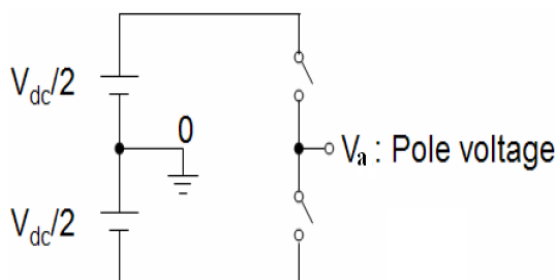


Fig.4 Circuit model of a single-phase inverter

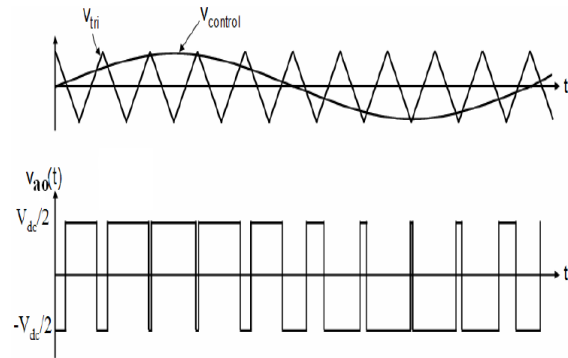


Fig.5 Pulse width modulation

The circuit model of a 3-phase voltage source PWM converter based STATCOM is given in Fig.4. It is of six power switches (IGBT based) as shown in that figure. When an upper IGBT is switched on, i.e. the output of the switches 1, 3, 5 is 1 and corresponding lower IGBT is switched off, the states of 4, 6, and 2 will be 0. Hence, there are eight possible combinations of on and off patterns of the switches and it produces eight inverter vectors ( $V_1$  to  $V_0$ ) as shown in Fig.7. Six are non-zero vectors ( $V_1$  to  $V_6$ ) and two are zero vectors ( $V_0$  and  $V_7$ ). It has been shown to generate less harmonic distortion in the output voltages and or currents applied to the phases of the load. It provides more efficient use of the DC-link voltage compared with sinusoidal pulse width modulation (SPWM) [15, 16-19] as illustrated in Fig.6.

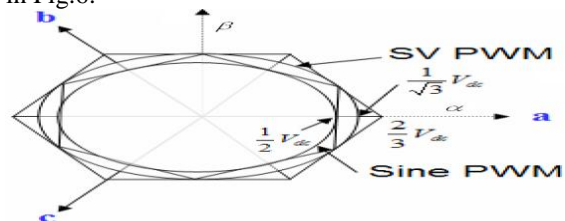


Fig.6 Locus of comparison of SVPWM over SPWM

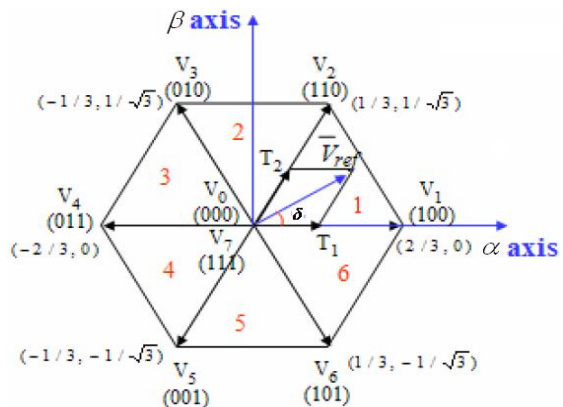


Fig.7 It shows the basic switching vectors and sectors

Switching time duration at any Sector

The switching times are derived using formula

$$T_1 = \frac{\sqrt{3} \cdot T_z \cdot |\bar{V}_{ref}|}{V_{dc}} \left( \sin \left( \frac{\pi}{3} - \delta + \frac{n-1}{3} \pi \right) \right) \quad (4)$$

And 
$$T_2 = \frac{\sqrt{3} \cdot T_z \cdot |\bar{V}_{ref}|}{V_{dc}} \left( \sin \left( \delta - \frac{n-1}{3} \pi \right) \right) \quad (5)$$

$T_0 = T_z - T_1 - T_2$ , where, n=1 through 6 (that is Sector 1 to 6) and  $0 \leq \delta \leq 60^\circ$  (6)

#### IV. MODELING OF THE STATCOM

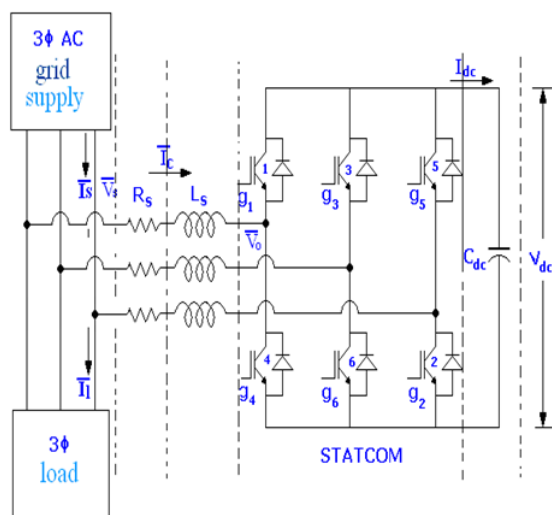


**Fig.8** Simplified main circuit diagram of the STATCOM

The ac side inductor,  $L_s$ , its inherent resistor,  $R_s$ , DC-link capacitor,  $C_{dc}$ , fundamental rms grid current,  $I_s$ , and load current,  $I_l$ , are shown in Fig.2.1. Three-phase grid voltage,  $v_{s,abc}$ , lags the STATCOM converter terminal voltages,  $v_{o,abc}$ , by phase angle difference,  $\alpha$ , This can be expressed as:

$$v_{s,abc} = \begin{bmatrix} v_{sa}(t) \\ v_{sb}(t) \\ v_{sc}(t) \end{bmatrix} = \sqrt{\frac{2}{3}} V_s \begin{bmatrix} \sin(\omega t - \alpha) \\ \sin\left(\omega t - \frac{2\pi}{3} - \alpha\right) \\ \sin\left(\omega t + \frac{2\pi}{3} - \alpha\right) \end{bmatrix} \quad (7)$$

The STATCOM current dynamics is governed by the following equation

$$L_s \frac{d}{dt} \begin{bmatrix} i_{ca}(t) \\ i_{cb}(t) \\ i_{cc}(t) \end{bmatrix} = -R_s \begin{bmatrix} i_{ca}(t) \\ i_{cb}(t) \\ i_{cc}(t) \end{bmatrix} + \begin{bmatrix} v_{sa}(t) \\ v_{sb}(t) \\ v_{sc}(t) \end{bmatrix} - \begin{bmatrix} v_{oa}(t) \\ v_{ob}(t) \\ v_{oc}(t) \end{bmatrix} \quad (8)$$

The zero-sequence component of current is always zero as

$$i_{ca}(t) + i_{cb}(t) + i_{cc}(t) = 0 \quad (9)$$

The balanced three-phase  $abc$  co-ordinate axes are directly transformed to orthogonal co-ordinate axes rotating at an angular speed  $\omega$  rad/sec are as follows:

$$\begin{bmatrix} x_d(t) \\ x_q(t) \\ x_o(t) \end{bmatrix} = K \begin{bmatrix} x_a(t) \\ x_b(t) \\ x_c(t) \end{bmatrix} \quad (10)$$

Where,

$$K = \sqrt{\frac{2}{3}} \begin{bmatrix} \sin(\omega t) & \sin\left(\omega t - \frac{2\pi}{3}\right) & \sin\left(\omega t + \frac{2\pi}{3}\right) \\ \cos(\omega t) & \cos\left(\omega t - \frac{2\pi}{3}\right) & \cos\left(\omega t + \frac{2\pi}{3}\right) \\ \frac{1}{\sqrt{2}} & \frac{1}{\sqrt{2}} & \frac{1}{\sqrt{2}} \end{bmatrix} \quad (11)$$

$[K]$  is square and nonsingular, hence invertible, so

$$[K]^{-1} = \sqrt{\frac{2}{3}} \begin{bmatrix} \sin(\omega t) & \cos(\omega t) & \frac{1}{\sqrt{2}} \\ \sin\left(\omega t - \frac{2\pi}{3}\right) & \cos\left(\omega t - \frac{2\pi}{3}\right) & \frac{1}{\sqrt{2}} \\ \sin\left(\omega t + \frac{2\pi}{3}\right) & \cos\left(\omega t + \frac{2\pi}{3}\right) & \frac{1}{\sqrt{2}} \end{bmatrix} = [K]^T \quad (12)$$

The relation between the grid voltage and STATCOM current in the resistor  $R_s$  gives

$$v_{s,abc}(t) = R_s i_{c,abc}(t) + v_{o,abc}(t) \quad (13)$$

The  $d-q$  transformation of above equation yields

$$v_{s,dqo}(t) = R_s i_{c,dqo}(t) + v_{o,dqo}(t) \quad (14)$$

The relationship between the grid voltage and STATCOM current in the series inductor  $L_s$  gives

$$L_s \frac{d}{dt} (i_{c,abc}(t)) = v_{abc}(t) - v_{o,abc}(t) \quad (15)$$

The  $d-q$  transformation of above equation yields,

$$L_s \frac{d}{dt} (i_{c,dqo}(t)) = L_s \frac{d}{dt} (K \cdot K^{-1} i_{c,dqo}(t) + v_{dqo}(t) - v_{o,dqo}(t)) \quad (16)$$

The dynamic equation of the STATCOM current is

$$L_s \frac{d}{dt} \begin{bmatrix} i_{cd}(t) \\ i_{cq}(t) \end{bmatrix} = \begin{bmatrix} -R_s & \omega L_s \\ -\omega L_s & -R_s \end{bmatrix} \begin{bmatrix} i_{cd}(t) \\ i_{cq}(t) \end{bmatrix} + \begin{bmatrix} v_{sd}(t) \\ v_{sq}(t) \end{bmatrix} - \begin{bmatrix} v_{od}(t) \\ v_{oq}(t) \end{bmatrix} \quad (17)$$

Under the assumption that harmonic components generated by the switching action in the converter are negligible, a switching function  $S$  can be defined as follow:

$$S = \begin{bmatrix} S_a(t) \\ S_b(t) \\ S_c(t) \end{bmatrix} = \sqrt{\frac{2}{3}} m_c \begin{bmatrix} \sin(\omega t) \\ \sin(\omega t - \frac{2\pi}{3}) \\ \sin(\omega t + \frac{2\pi}{3}) \end{bmatrix} \quad (18)$$

The modulation index, being constant for a programmed PWM, is given by

$$MI = m = \frac{v_{o,peak}}{v_{dc}} = \sqrt{\frac{2}{3}} m_c \quad (19)$$

Where,  $m_c$  is called as modulation conversion

index(MCI) and  $\sqrt{\frac{2}{3}}$  is the multiplying factor for the

transformation of three-phase stationary  $abc$  axes to rotating  $d - q$  quantities

The STATCOM converter terminal phase voltages are given by

$$v_{o,abc}(t) = S v_{dc}(t) \quad (20)$$

The STATCOM converter terminal phase voltages in  $d - q$  frame with (10) and (20) are given as

$$v_{o,dq} = K S v_{dc} = m_c \begin{bmatrix} 1 \\ 0 \end{bmatrix} v_{dc}(t) \quad (21)$$

On solving equation (17) by using transformation method and equation(21), the  $d - q$ -axis currents of the STATCOM are

$$\frac{d}{dt} \begin{bmatrix} i_{cd}(t) \\ i_{cq}(t) \end{bmatrix} = \begin{bmatrix} -\frac{R_s}{L_s} & \omega \\ \omega & -\frac{R_s}{L_s} \end{bmatrix} \begin{bmatrix} i_{cd}(t) \\ i_{cq}(t) \end{bmatrix} + \frac{1}{L_s} \begin{bmatrix} V_s \cos \alpha - m_c v_{dc}(t) \\ -V_s \sin \alpha \end{bmatrix} \quad (22)$$

The DC side capacitor current of the STATCOM and its  $d - q$  axis current is given as

$$i_{dc}(t) = S^T i_{c,abc}(t) \quad (23)$$

$$i_{dc}(t) = S^T K^{-1} \begin{bmatrix} i_{cd}(t) \\ i_{cq}(t) \end{bmatrix} = m_c \begin{bmatrix} 1 & 0 \end{bmatrix} \begin{bmatrix} i_{cd}(t) \\ i_{cq}(t) \end{bmatrix} \quad (24)$$

The relationship between the voltage and current in the DC side of the STATCOM is given by:

$$i_{dc}(t) = C_{dc} \frac{dv_{dc}(t)}{dt} \quad (25)$$

Replacing (25) in (24), the DC link voltage dynamic equation of the STATCOM is

$$\frac{dv_{dc}(t)}{dt} = \frac{m_c}{C_{dc}} i_{cd}(t) \quad (26)$$

Replacing (26) in (25), the complete mathematical model of the STATCOM in  $d - q$ -axis will be as follows:

$$\frac{d}{dt} \begin{bmatrix} i_{cd}(t) \\ i_{cq}(t) \\ v_{dc}(t) \end{bmatrix} = \begin{bmatrix} -\frac{R_s}{L_s} & \omega & -\frac{m_c}{L_s} \\ \omega & -\frac{R_s}{L_s} & 0 \\ \frac{m_c}{C_{dc}} & 0 & 0 \end{bmatrix} \begin{bmatrix} i_{cd}(t) \\ i_{cq}(t) \\ v_{dc}(t) \end{bmatrix} + \frac{V_s}{L_s} \begin{bmatrix} \cos \alpha \\ -\sin \alpha \\ 0 \end{bmatrix} \quad (27)$$

The active and reactive powers injected or drawn by the STATCOM are expressed in equation (28) and (29) respectively.

$$p_c(t) = v_{sd}(t) i_{cd}(t) + v_{sq}(t) i_{cq}(t) = -V_s i_{cd}(t) \cos \alpha + V_s i_{cq}(t) \sin \alpha \quad (28)$$

$$q_c(t) = v_{sq}(t) i_{cd}(t) - v_{sd}(t) i_{cq}(t) = -V_s i_{cd}(t) \sin \alpha - V_s i_{cq}(t) \cos \alpha \quad (29)$$

The states of  $I_{cd}(s)$ ,  $I_{cq}(s)$  and  $V_{dc}(s)$  of the STATCOM can be extricated in frequency domain from (30), expressed as:

$$I_{cd}(s) = \frac{V_s \left[ s^2 \frac{\cos \alpha}{L_s} + s \left( \frac{R_s}{L_s} \cos \alpha - \frac{\omega}{L_s} \sin \alpha \right) \right]}{s^3 + 2s^2 \frac{R_s}{L_s} + s \left( \omega^2 + \frac{R_s^2}{L_s^2} + \frac{m_c^2}{L_s C_{dc}} \right) + m_c^2 \frac{R_s}{L_s^2 C_{dc}}} \quad (30)$$

$$I_{cq}(s) = \frac{-V_s \left[ s^2 \frac{\sin \alpha}{L_s} + s \left( \frac{R_s}{L_s} \sin \alpha + \frac{\omega}{L_s} \cos \alpha \right) + \frac{m_c}{L_s C_{dc}} \sin \alpha \right]}{s^3 + 2s^2 \frac{R_s}{L_s} + s \left( \omega^2 + \frac{R_s^2}{L_s^2} + \frac{m_c^2}{L_s C_{dc}} \right) + m_c^2 \frac{R_s}{L_s^2 C_{dc}}} \quad (31)$$

$$V_{dc}(s) = m_c V_s \frac{\left[ s \frac{\cos \alpha}{L_s C_{dc}} + \frac{R_s}{L_s^2 C_{dc}} \cos \alpha - \frac{\omega}{L_s C_{dc}} \sin \alpha \right]}{s^3 + 2s^2 \frac{R_s}{L_s} + s \left( \omega^2 + \frac{R_s^2}{L_s^2} + \frac{m_c^2}{L_s C_{dc}} \right) + m_c^2 \frac{R_s}{L_s^2 C_{dc}}} \quad (32)$$

## V. ANALYSIS

A small signal model has been proposed in [20] to model the STATCOM for varying  $\alpha$  and/or  $m$  ( $m_c$ ). In their model [20], the authors did not make use of the dependence of  $\alpha$  on  $m$  ( $m_c$ ), both

of which play important roles in the STATCOM dynamics. An improved model, referred to in this paper as the “first small signal model” (Model II) is proposed in this present work, making use of the relationship between  $\alpha$  and  $m$  ( $m_c$ ).

For a given operating point, Model II of the STATCOM is derived on the basis of the following assumptions [20, 21]:

- ❖ The second and other higher order terms (products of variations) are negligible.
- ❖ The change  $\hat{\alpha}$  is small.

With the above assumptions, the  $d$ -axis component  $v_{od}$  [equation (21)] may be written as:

$$V_{od} + \hat{v}_{od}(t) = (M_c + \hat{m}_c(t))(V_{dc} + \hat{v}_{dc}(t)) \quad (33)$$

At steady state  $V_{od} = M_c V_{dc}$  giving us,

$$\hat{v}_{od}(t) = M_c \hat{v}_{dc}(t) + \hat{m}_c(t) V_{dc} \quad (34)$$

At the same time the DC-link current of the STATCOM given by equation (24) may be rewritten as:

$$I_{cd} + \hat{i}_{cd}(t) = (M_c + \hat{m}_c(t))(I_{cd} + \hat{i}_{cd}(t)) \quad (35)$$

At steady state  $I_{cd} = 0$ , which gives,

$$\hat{i}_{cd}(t) = M_c \hat{i}_{cd}(t), \text{ neglecting higher order variations}$$

$$\text{Or, } C_{dc} \frac{d}{dt} \hat{v}_{dc}(t) = M_c \hat{i}_{cd}(t) \quad (36)$$

where the variables with ‘hats’ are small variations over the steady state values. For small values of  $\hat{\alpha}$  (small perturbations) the values of sine and cosine functions may be approximated by:

$$\sin \hat{\alpha} \approx \hat{\alpha}, \cos \hat{\alpha} \approx 1 \quad (37)$$

Applying the same assumptions to equations (16), the small signal equations are

$$L_s \frac{d}{dt} (\hat{i}_{cd}(t)) = \omega_1 L_s \hat{i}_{cq}(t) - R_s \hat{i}_{cd}(t) - M_c \hat{v}_{dc}(t) - \hat{m}_c(t) V_{dc} \quad (38)$$

$$L_s \frac{d}{dt} (\hat{i}_{cq}(t)) = -R_s \hat{i}_{cq}(t) - \omega_1 L_s \hat{i}_{cd}(t) - V_s \hat{\alpha}(t) \quad (39)$$

Taking Laplace Transform, the states of  $\hat{I}_{cd}$ ,  $\hat{I}_{cq}$ ,  $\hat{V}_{dc}$  can be determined as

$$\begin{bmatrix} \hat{I}_{cd}(s) \\ \hat{I}_{cq}(s) \\ \hat{V}_{dc}(s) \end{bmatrix} = \frac{1}{A(s)} \begin{bmatrix} s^2 L_s C_{dc} + s R_s C_{dc} & s \omega_1 L_s C_{dc} & -s M_c L_s - M_c R_s \\ -s \omega_1 L_s C_{dc} & s^2 L_s C_{dc} + s R_s C_{dc} + M_c^2 & M_c \omega_1 L_s \\ s M_c L_s + M_c R_s & M_c \omega_1 L_s & (s L_s + R_s)^2 + (\omega_1 L_s)^2 \end{bmatrix} \begin{bmatrix} -V_{dc} \hat{m}_c(s) \\ -V_s \hat{\alpha}(s) \\ 0 \end{bmatrix} \quad (40)$$

Where,

$$A(s) = L_s^2 C_{dc} s^3 + 2 L_s C_{dc} R_s s^2 + [C_{dc} R_s^2 + (\omega_1 L_s)^2 + M_c^2 L_s] s + M_c^2 R_s$$

Transfer functions connecting the signals can be derived as:

$$\frac{\hat{I}_{cd}(s)}{\hat{m}_c(s)} = \frac{-V_{dc} C_{dc} (s L_s + R_s)}{A(s)}$$

$$\frac{\hat{I}_{cd}(s)}{\hat{\alpha}(s)} = \frac{-V_{dc} \omega_1 L_s C_{dc} s}{A(s)} \quad (41)$$

$$\frac{\hat{I}_{cq}(s)}{\hat{m}_c(s)} = \frac{s V_{dc} \omega_1 L_s C_{dc}}{A(s)}$$

$$\frac{\hat{I}_{cq}(s)}{\hat{\alpha}(s)} = \frac{-V_s (L_s C_{dc} s^2 + R_s C_{dc} + M_c^2)}{A(s)} \quad (42)$$

$$\frac{\hat{V}_{dc}(s)}{\hat{m}_c(s)} = \frac{-M_c V_{dc} (s L_s + R_s)}{A(s)}$$

$$\frac{\hat{V}_{dc}(s)}{\hat{\alpha}(s)} = \frac{-M_c V_s \omega_1 L_s}{A(s)} \quad (43)$$

The responses of the states  $\hat{i}_{cq}$ ,  $\hat{i}_{cd}$  and  $\hat{v}_{dc}$  (as in (2.29-2.31)) are simulated in MATLAB (using the parameters given in Table-A.1) with a step variation of  $\hat{\alpha} = -5^\circ$  and a change of  $\hat{m} = 0.08164$  ( $\hat{m}_c = 0.1$ ). It however causes  $V_{dc}$  to reduce by 35 V in the steady state as shown in Fig.9(b). However, due to a change in  $\hat{\alpha}$ , the STATCOM draws additional steady state reactive current of 37 A (Fig.10(a)) at steady state. Neither does,  $v_{dc}$ , the DC-link voltage remain at its previous steady state value. It increases in magnitude (by 50 V) for a change in  $\hat{\alpha}$  (Fig.10(b)). Hence the open loop dynamics suggest that closed-loop control is required for reactive component of the STATCOM current as well as  $v_{dc}$  in order to reduce transient surges and to keep  $V_{dc}$  constant.

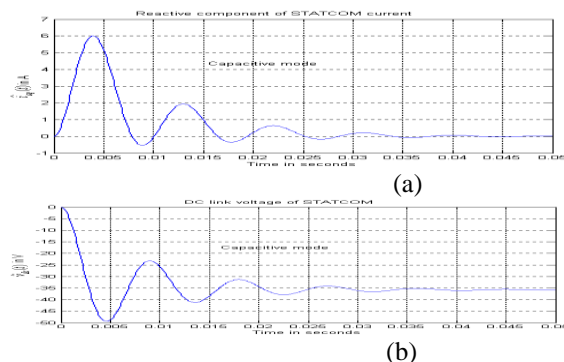


**Fig.9** Transient response in Model II for a small change in  $\hat{m}_c = 0.1$  ( $\hat{m} = 0.8164$ ) in capacitive mode: (a)  $\hat{i}_{cq}$  w.r.t. time and (b)  $\hat{v}_{dc}$  w.r.t. time

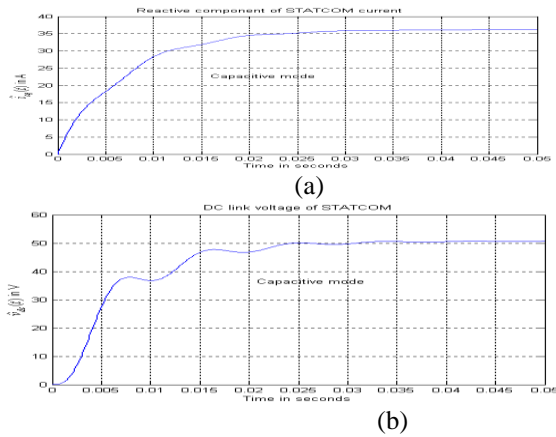


**Fig.10** Transient response in Model II for a small change in  $\hat{\alpha}$  ( $-5^\circ$ ) in capacitive mode: (a)  $\hat{i}_{cq}$  w.r.t. time and (b)  $\hat{v}_{dc}$  w.r.t. time.

**VI. CONTROLLER DESIGN**

To achieve a fast dynamic response of the STATCOM, it is required that the  $V_{dc}$ , be kept constant by controlling  $\hat{\alpha}$  and  $\hat{m}$  ( $\hat{m}_c$ ). Simultaneously the load reactive power may be compensated by controlling  $\hat{\alpha}$  only.

If the  $V_{dc}$  is to be kept constant, then the variation  $\hat{V}_{dc}$  should be zero. Hence, from equation (26)

Putting  $\hat{V}_{dc} = 0$ ,  

$$\Rightarrow \hat{m}_c(s) = -\frac{V_s \omega_1 L_s}{V_{dc} (sL_s + R_s)} \hat{\alpha}(s) = G_{m2a} \hat{\alpha}(s) \quad (44)$$

Where,  $G_{m2a} = \frac{-V_s \omega_1 L_s}{V_{dc} (sL_s + R_s)} \quad (45)$

By using above relation I have proposed a block diagram of the closed-loop control system with a PI-controller in order to control the reactive component of the STATCOM current. It is noteworthy that this would indirectly control the DC-link voltage.

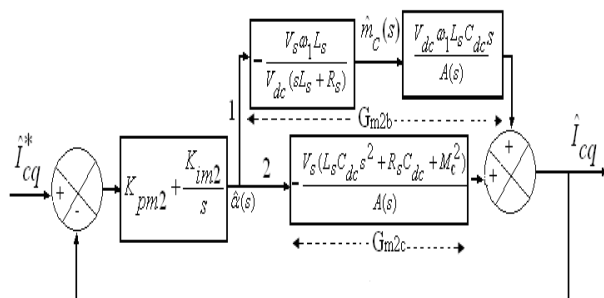


**Fig.11** Closed-loop block diagram with PI-controller for Model II

The transfer functions (open-loop,  $G_{m2o}$  and closed-loop,  $G_{m2}$ ) between the reference reactive current to the generated reactive current of the STATCOM are

$$G_{m2o} = G_{pi} (G_{m2b} + G_{m2c}) \quad (46)$$

$$G_{m2} = \frac{G_{pi} (G_{m2b} + G_{m2c})}{1 + G_{pi} (G_{m2b} + G_{m2c})} \quad (47)$$

$\tau$  is chosen to be 3.3m sec. The parameters of PI-controller (47) are determined by the root locus method (taking  $\xi = 0.25$ ) and their values are determined after inserting the values of the system parameters from Table-A.1.

$$K_{pm2} = -0.02 \text{ rad / A}, K_{im2} = -6.66 \text{ sec}$$

The simulation of the step response of the above closed-loop control scheme is shown in Fig.12. It may be noted that the unit step response of  $\hat{i}_{cq}$  settles at 12m sec with only 5% overshoot (Fig.12(a)). These controller parameters are also applied to the same closed-loop system for checking the tracking transients of the STATCOM. From Fig.12 (b), it may be further noted that the STATCOM can track the reference reactive current of  $\mp 20$  A in both capacitive and inductive mode. The output settles at 1m sec with overshoot of only 2 A in both modes.

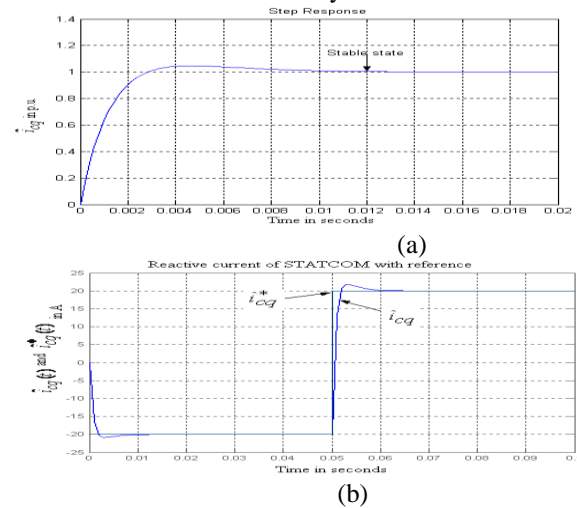


**Fig.12** Response of  $\hat{i}_{cq}$  of the STATCOM with PI-controller for Model II: (a) Step response and (b) with actual  $\hat{i}_{cq}$

Sl.No	Meaning	Symbol	Values
1	Fundamental frequency	$f = f_1$	50 Hz
2	Fundamental angular frequency	$\omega = \omega_1$	314 rad/sec
3	RMS line-to-line voltage	$V_s$	415V

4	Effective coupling resistance of inductor	$R_s$	1.0 $\Omega$
5	Coupling inductance or ac side reactor	$L_s$	5.44mH
6	DC-link capacitor	$C_{dc}$	680 $\mu F$
7	Modulation index (Modulation conversion index)	$m (m_c)$	0.866 to 1.00 (0.979 to 1.22)
8	Load resistance	$R_l$	23 $\Omega$
9	Load inductance(with its inherent resistance)	$L_l (r_l)$	60 mH (2.06 $\Omega$ )

Table-A.1: Parameters and variables of the STATCOM system

### VII. SIMULATION BLOCK

In this paper, STATCOM is implemented which will control q-axis current using MATLAB/SIMULINK.

Here 23  $\Omega$  and 60mH is taken as load  
 Switching frequency=10 KHz

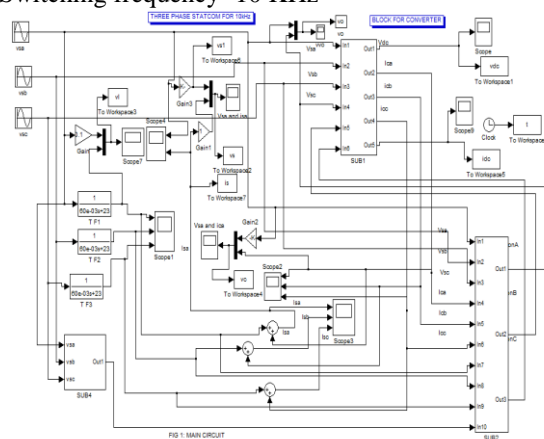


Fig.13.Total simulink block

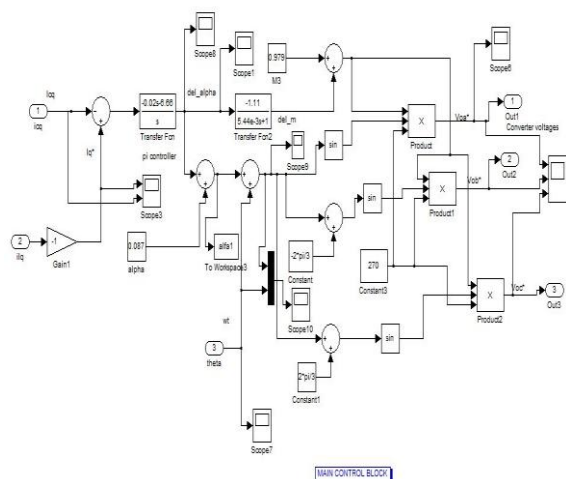


Fig.14.main controller simulink block

### VIII. SIMULATION RESULTS

The waveforms of the grid side phase-a voltage ( $v_{sa}$ ) and current ( $i_{sa}$ ) at point of common connection (PCC) (without the STATCOM in operation) are shown in Fig.15.  $v_{sa}$  is plotted to a reduced scale of 10 : 1 .

steady state it is seen that the power angle is  $39.64^\circ$  (so that power factor is 0.77) . The STATCOM will now act in closed-loop with this system along with the proposed controllers in order to improve this power factor.

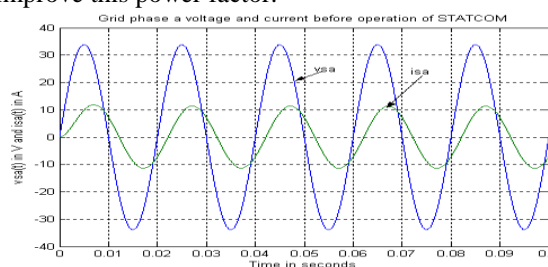


Fig.15 Grid phase-a voltage and current with  $R - L$  load before operation of the STATCOM  
 Operation with controller :

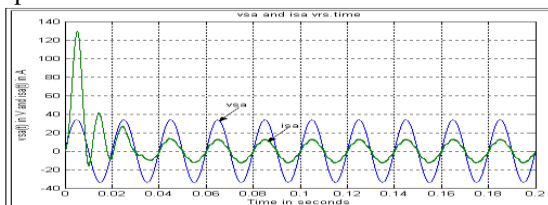


Fig.16 System voltage and system current after Compensation at DC link capacitor voltage of 100V

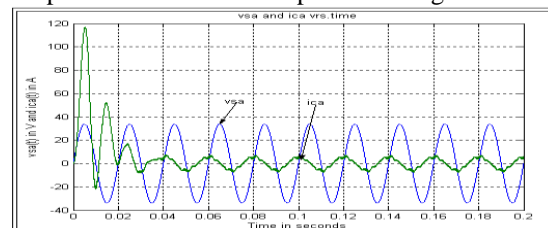


Fig.17 System voltage and STATCOM current at DC link capacitor voltage of 100V

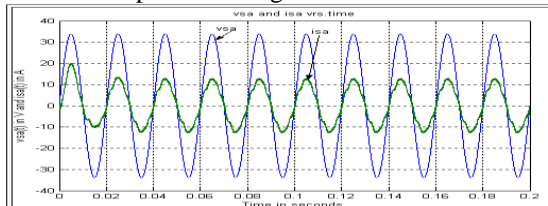
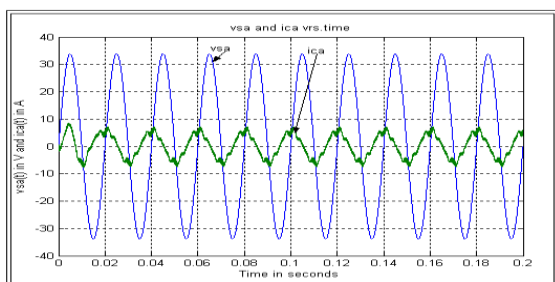
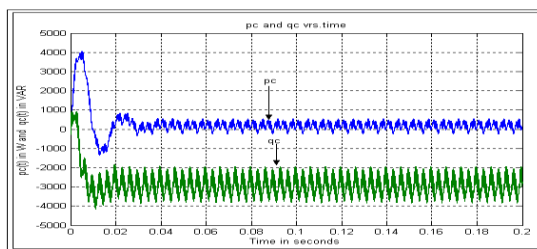


Fig.18 System voltage and system current after compensation at DC link voltage of 550V



**Fig.19** System voltage and STATCOM current at DC link voltage of 550V



**Fig.20** Active and reactive power generated by STATCOM

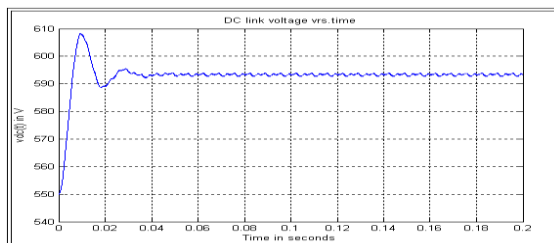


**Fig.21** DC link voltage

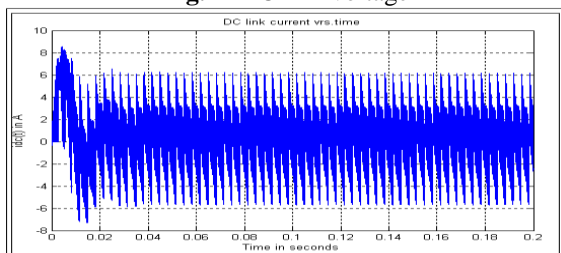


**Fig.22** DC link current

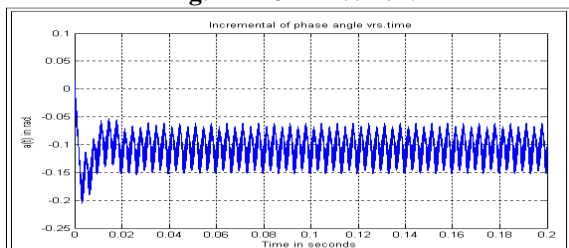


**Fig.23** Variation of incremental of phase angle

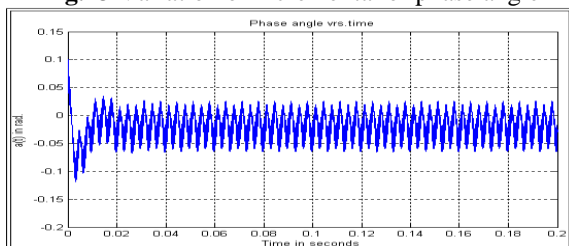


**Fig.24** Variation of phase angle

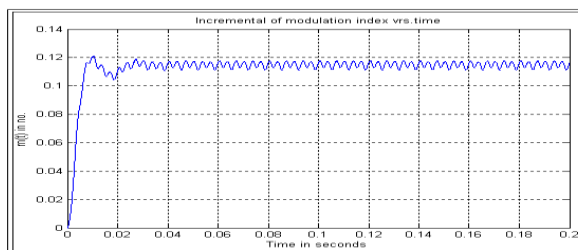


**Fig.25** Variation of incremental of modulation index

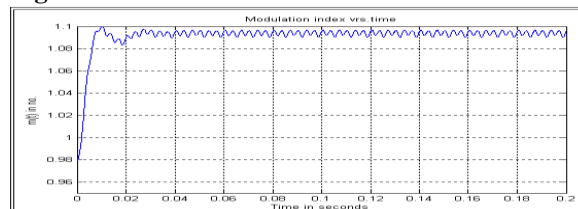


**Fig.26** Variation of modulation index

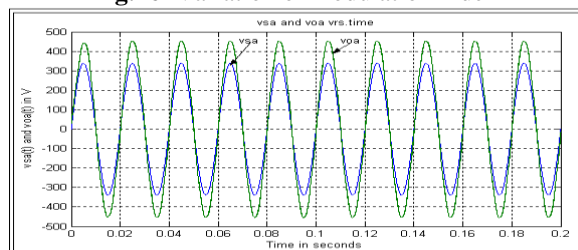


**Fig.27** System voltage and STATCOM output voltage

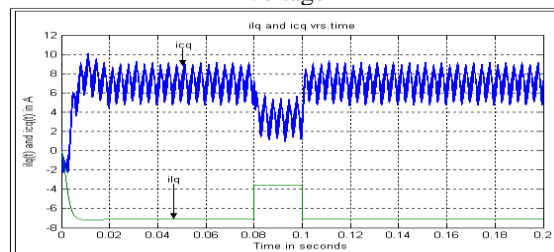


**Fig.28** With change of load reactive current and STATCOM reactive current

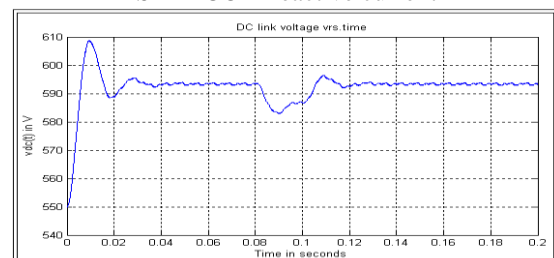


**Fig.29** DC voltage with change of reference

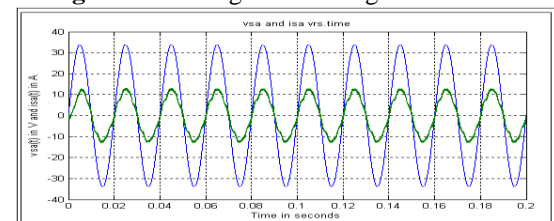


**Fig.30** System voltage and system current at 600V DC link capacitor voltage

## IX. CONCLUSION

In this paper, a small signal model of the STATCOM is proposed considering the grid voltage to be lagging to the fundamental component of the STATCOM converter output voltage. There is no separately designed controller for the DC-link voltage for the strategy of STATCOM. The strategy has been simulated using MATLAB/SIMULINK environment for different pre-charge voltage on the DC-link, with linear load. The STATCOM is applied for improving the power factor of the grid current in this case.

## REFERENCE

- [1] C.L.Wadhwa, "Electrical Power Systems", Wiley Eastern Ltd, New Delhi, 1995.
- [2] E.W.Kimberk, "Power System Stability Vol.I, II, III", Wiley Eastern Ltd, New Delhi, 1994.
- [3] P.M.Anderson and A.A.Fouad, "Power System Control and Stability", Iowa State, University Press, Ames, Iowa, 1997.
- [4] P.Kundur, "Power System Stability and Control", EPRI, Power Engineering Series, 1994.
- [5] C.W.Taylor, "Power System Voltage Stability", McGraw-Hill, 1994.
- [6] S.Mark Halpin and R.F.Burch, "An Improved Simulation Approach for the Analysis of Voltage Flicker and the Evaluation of Mitigation Strategies", IEEE Transactions on Power Delivery, Vol.12, No.3, pp.1285-1291, July 1997.
- [7] M.F.McGranaghan, D.R.Mueller and M.J.Samotyj, "Voltage Sags in Industrial Systems", IEEE Transactions on Industry Applications, Vol.29, No.2, pp.397-403, March/April 1993.
- [8] C.J.Melborn, T.D.Davis and G.E.Beam, "Voltage sags: Their Impact on the Utility and Industrial Customers", IEEE Transactions on Industry Applications, Vol.34, No.3, pp.549-557, May/June 1998.
- [9] M.K.Pal, "Voltage Stability Conditions Considering Load Characteristic", IEEE Transactions on Power Systems, Vol.7, No.1, pp.243-249, Feb.1992.
- [10] M.K.Pal, "Voltage Stability: Analysis needs, modeling requirement, and modeling adequacy", IEE Proceedings-C, Vol.140, No.4, pp.279-286, July 1993.
- [11] T.V.Cutsem and C.D.Vournas, "Voltage Stability analysis in transient and mid-term time scales", IEEE Transactions on Power Systems, Vol.11, No.1, pp.146-154, Feb.1994.
- [12] T.J.E.Miller, "Reactive Power Control in Electric Systems" John Wiley, 1982.
- [13] K.R.Padiyar, "Power System Dynamics-Stability and Control", Interline Publishing Ltd, Bangalore, 1996.
- [14] Y.H. Song and A.T.John "Flexible AC Transmission Systems (FACTS)", IEE Power and Energy series Inc. 1999.
- [15] B.K.Bose, "Modern Power Electronics and Drives", Prentice-Hall, Inc.2002.
- [16] R.Wu, S.B.Dewan and G.R.Slemon, "Analysis of an ac-to-dc Voltage Source Converter Using PWM with Phase and Amplitude Control", IEEE Transactions on Industry Applications, Vol.27, No.2, pp.355-363, March/April 1991.
- [17] K.Zhou and D.Wang, "Relation between Space Vector Modulation and Three Phase Carrier- Based PWM: A Comprehensive Analysis", IEEE Transactions on Industrial Electronics, Vol.49, No.1, pp.186-196, Feb. 2002.
- [18] A.Kwasinski, P.T.Krein and P.L.Chapman, "Time Domain Comparison of Pulse-Width Modulation Schemes", IEEE Power Electronics Letters, Vol.1, No.3, pp.64-68, Sept. 2003.
- [19] S.K.Mondal, B.K.Bose, V.Oleschuk and J.O.Pinto, "Space Vector Pulse Width Modulation of Three-Level Inverter Extending Operation into Over modulation Region", IEEE Transactions on Power Electronics, Vol.18, No.2, pp.604-611, March 2003.
- [20] G.C. Cho, N.S. Choi, C.T. Rim and G.H. Cho, "Modeling, Analysis and Control of Static Var Compensator using Three-Level Inverter", IEEE, Industry Society Meet, pp.837-843, 1992.
- [21] J.K.Moharana, M.Sengupta, A.Sengupta "Closed-Loop Control of a lab-scale STATCOM prototype for Reactive Power Compensation", communicated to NPEC-2011, BESU, Shibpur, Howrah, West Bengal, 2011.